Plasmon-phonon coupling in δ-doped polar semiconductors

Guo-Qiang Hai, Nelson Studart, and Gilmar E. Marques
Departamento de Física, Universidade Federal de São Carlos, 13565-905 São Carlos, São Paulo, Brazil
(Received 28 May 1996; revised manuscript received 3 September 1996)

The collective excitations and their coupling to optical phonons have been studied for a two-dimensional electron gas in δ-doped polar semiconductors within the random-phase approximation. Our calculation shows that, due to the high electron density in these systems in which several subbands are occupied, both intrasubband and intersubband plasmon modes are strongly coupled to the optical-phonon modes. [S0163-1829(97)06204-8]

I. INTRODUCTION

The quasi-two-dimensional (Q2D) electron gas system in δ-doped semiconductor structure is realized by producing a very thin doping layer with high impurity concentration. Because the dopants are confined to a single or few monolayers of the semiconductor lattice, the doping profile can be mathematically described by Dirac's δ function. Semiconductors with such dopant distributions are referred to as δ-doped semiconductors.[1] The incorporation of dopants within a few monolayers leads to electron confinement in the space-charge potential well and thus to a set of subbands where the electron motion perpendicular to the doping layer is quantized. It presents an important Q2D semiconductor system in which high electron densities are attained and several subbands are occupied leading to a new multisubband system. The electron confinement in δ-doped semiconductors is simply realized by a space-charge potential well. So, the subband energy E_n and the wave function $\psi_n(z)$ are obtained from the numerical solution of the coupled one-dimensional Poisson and Schrödinger equations. If we take the doping layer in the xy plane located at $z=0$, the confinement potential of the system is symmetric about the $z=0$ plane. The total electron energy and wave function are given by

$$E_n(\vec{k}) = E_n + \varepsilon(\vec{k}) \tag{1}$$

and

$$\Psi_{n,\vec{k}}(\vec{r},z) = \psi_n(z)\frac{1}{\sqrt{A}}\exp(i\vec{k}\cdot\vec{r}), \tag{2}$$

where $n=1, 2,\ldots$ is the subband index, $\vec{r}$ ($\vec{k}$) the electron position (wave vector) in the xy plane, $\varepsilon(\vec{k})=\hbar^2k^2/2m^*$ the electron kinetic energy, m^* the electron effective mass, and A the area of sample.

Since the pioneering experimental work by Bass,[2] Wood *et al.*,[3] and Schubert *et al.*,[4] highly spatially confined impurity doping layers have been achieved in semiconductors by the molecular-beam epitaxy technique. A large number of experimental investigations[1,5–11] have been carried out on the electron transport and optical properties in δ-doped semiconductors. Furthermore, novel and improved semiconductor devices have been fabricated from δ-doped structures, such as δ-doped doping-superlattice light-emitting diodes,[12] lasers,[13] and modulators,[14] high-transconductance selectively δ-doped heterostructure transistors,[15] planar-doped barrier diodes,[16] negative differential conductance oscillators,[17] etc.

Plasma excitations in low-dimensional electron systems have been studied extensively.[18] As proposed by Burnstein *et al.*,[19] resonant inelastic light scattering is a sensitive method for the investigation of the elementary excitations in 2D electron systems. It yields separate spectra of single-particle and collective excitations, which leads to the determination of the energy states and collective electron-electron interaction. This yields substantial information on different 2D semiconductor systems. Plasmons in semiconductor superlattices have also attracted much attention.[20–26] Novel collective modes have been found in artificially structured superlattices. Das Sarma[27] presented a generalized many-body dielectric theory to study the spectrum of collective excitations in Q2D electron systems realized in semiconductor heterostructures. The intersubband plasmon modes and their coupling to the intrasubband plasmon modes also were investigated.[27–29] It was shown that the resonant mode coupling of intersubband and intrasubband plasmons takes place in an asymmetric quantum well at high electron densities and small energy separation between the subbands. Backes *et al.*[30] investigated the effects of confinement on the plasmon modes in the Q2D system. By including all the energy levels in an infinite quantum well, they recovered the results of the ideal 2D and 3D electron systems by varying the width of the quantum well from zero to infinity.

Collective excitations and their coupling to the longitudinal-optical (LO) phonons in doped polar semiconductor structures are the basic physical phenomena which affect the different aspects of the electronic and optical properties of the systems.[18] Wu, Peeters, and Devreese[31] studied the plasmon-phonon coupling of 2D electron electron gas in $GaAs/Al_xGa_{1-x}As$ heterojunctions. They showed that the intrasubband plasmon mode in GaAs heterostructures is strongly coupled to the LO phonon modes at high electron densities. When the unperturbed plasmon frequency is close to the LO-phonon frequency, a resonant coupling takes place and there is a splitting of the plasmon frequency. Wendler and Pechstedt[32] investigated interface effects on the phonon modes and the plasmon-phonon coupling in a semiconductor quantum well. They found that the Landau damping of the intersubband plasmon modes depends strongly on the width of the quantum well and the electron density. The δ-doped

polar semiconductors, e.g., Si δ-doped GaAs, have also several advantages to study the collective excitations and their coupling to LO phonons. The electron density in δ-doped semiconductors is much higher than the other Q2D systems, such as heterojunctions and quantum wells, in which electron-electron interactions play a substantial role. It could be a good system to investigate the electron-electron interaction for a deeper understanding of the many-body effects. Typically, several subbands are occupied in δ-doped semiconductors, so the intersubband interaction is strong. Furthermore, the separation between the different subbands is close to the optical phonon energy in such a way that the electron LO-phonon coupling is strong and easier to be detected experimentally. On the other hand, the host semiconductor is uniform in such a way that there is no material interface present. The phonon modes in δ-doped systems have, therefore, a three-dimensional character. The electron-phonon interaction can be described by the Fröhlich Hamiltonian. This is different from other Q2D systems, such as $GaAs/Al_xGa_{1-x}As$ heterostructures, where the interface modifies the phonon modes, and consequently, the electron-phonon interaction. In this case, the Fröhlich Hamiltonian is only a good approximation to describe the electron-phonon interaction when the interface effects are not pronounced.[33]

In our previous works,[34–36] we studied the electron transport properties in δ-doped semiconductors. The effects due to intersubband coupling and screening of the Q2D electron gas on the ionized impurity scattering were investigated theoretically. The subband transport and quantum mobilities coming from ionized impurity scattering were analyzed. We found that not only the intersubband scattering by itself, but also the intersubband coupling through the screening of the Q2D electron gas plays an essential role in the electron transport in this multisubband system.

In this paper, we study the spectrum of collective excitations of a Q2D electron gas in δ-doped polar semiconductors. Our model consists of a multisubband 2D electron gas system coupled to 3D bulk optical phonons at zero temperature. The intrasubband and intersubband plasmon modes and their coupling to the optical phonons are investigated. Our calculation is based on the dielectric function in the random-phase approximation (RPA) and is applied to Si δ-doped GaAs structure of an impurity layer in the xy plane with thickness $W_D = 10$ Å. The electronic structure is determined by employing a self-consistent method within the local density approximation.[35] We assumed that all the donors in the doping layer are ionized and the background acceptor concentration, which is supposed to be uniformly distributed in the sample, is $n_A = 10^{15}$ cm^{-3}. We found that in the present system the $n = 2$, 3, and 4 subbands begin to be occupied at the total electron density $N_e = 0.93$, 2.67, and 8.33×10^{-12} cm^{-2}, respectively.

Experimentally, Mlayah *et al.*[9] investigated the intersubband plasmon-phonon coupling in Si δ-doped GaAs. The signature of the coupled modes was pointed out by means of Raman scattering measurements. They found that the phononlike mode, due to the coupling of the intersubband plasmon of the lowest two subbands to the LO phonons, is located between LO and TO phonon frequencies. Influences of the doping concentration and thickness of the doping layer on these phononlike modes were discussed.

According to the experimental accessible electron densities, we consider a realistic four-subband model, and in order to make our discussion clearer, we analyze first the case where one subband is occupied and the other three are empty. Second, we discuss the results when electrons occupy two subbands and the other ones are empty, and finally the case where three subbands are occupied. Our calculation shows that both the intersubband plasmon modes and their coupling to the LO phonons are much more pronounced in δ-doped polar semiconductors than those in other Q2D semiconductor systems. In a wide range of electron densities (donor concentrations), the frequencies of the phononlike branches of the intersubband plasmon-phonon modes due to the first four subbands are in the reststrahlen region of GaAs.

We do not consider impurity scattering effects on the plasmon excitation spectrum. Such scattering should be strong in the δ-doped system and soften the plasmon spectrum. It may also lead to a mixture of different plasmon modes when they are close to each other. But the main features shown in this work will not be modified essentially. As far as we know, this is the first theoretical work studying the collective excitations and their coupling to LO phonons in δ-doped semiconductors.

II. PLASMON-PHONON COUPLING

For an electron gas embedded in a polar semiconductor, the optical phonons interact with the electrons. Since the host material of the 2D electron gas in the δ-doped system is homogeneous, which is different from the other 2D systems such as heterojunctions and quantum wells where interfaces between different materials are present, the electron-phonon interaction can be described by the well-known Fröhlich Hamiltonian. The electrons interact among themselves through the Coulomb interaction and through the virtual LO phonons via the Fröhlich interaction. In this way, both the electron-electron interaction and the electron-phonon interaction play significant roles and affect substantially the electron and the phonon systems.[37] Especially, the electron-phonon coupling may be strong because the intersubband plasmon frequencies in Si δ-doped GaAs are close to the optical phonon frequency.

In a Q2D system, the screened interaction potential $V^{sc}_{nn',mm'}(\vec{q},\omega)$ within the RPA is determined by the Dyson equation[37]

$$V^{sc}_{nn',mm'}(\vec{q},\omega) = V_{nn',mm'}(\vec{q},\omega) + \sum_{ll'} V_{nn',ll'}(\vec{q},\omega) \times \Pi^0_{ll'}(\vec{q},\omega) V^{sc}_{ll',mm'}(\vec{q},\omega), \qquad (3)$$

where $V_{nn',mm'}(\vec{q},\omega) = v^c_{nn',mm'}(\vec{q}) + v^{ph}_{nn',mm'}(\vec{q},\omega)$ is the bare interaction potential which is composed by the electron-electron Coulomb potential and the electron-phonon interaction determined by the Fröhlich Hamiltonian, and $\Pi^0_{mm'}(\vec{q},\omega)$ is the polarizability function of the noninteracting 2D electron gas. The well-known bare electron-electron potential is[38]

$$v^{c}_{nn',mm'}(\vec{q})=\frac{2\pi e^2}{\epsilon_\infty q}F_{nn',mm'}(q), \tag{4}$$

with the Coulomb form factor

$$F_{nn',mm'}(q)=\int_{-\infty}^{\infty}dz\,\psi_n(z)\psi_{n'}(z)\times\int_{-\infty}^{\infty}dz'\,\psi_m(z')\psi_{m'}(z')e^{-q|z-z'|}. \tag{5}$$

Due to the spatial symmetry of the potential about the $z=0$ plane, which is a characteristic of the δ-doped system, we have

$$F_{nn',mm'}(q)=F_{n'n,mm'}(q)=F_{nn',m'm}(q)=F_{n'n,m'm}(q).$$

Furthermore, the Coulomb form factor $F_{nn',mm'}(q)$ vanishes if $n+n'+m+m'$ is an odd number. Notice that $F_{nn',mm'}(0)=1$ for $n=n'$ and $m=m'$, and $F_{nn',mm'}(0)=0$ otherwise.

The bare electron-phonon interaction coming from the Fröhlich Hamiltonian is given by

$$v^{\rm ph}_{nn',mm'}(\vec{q},\omega)=\frac{2\omega_{\rm LO}}{\hbar(\omega^2-\omega^2_{\rm LO})}\sum_{q_z}M_{nn'}(\vec{q},q_z)\times M^{*}_{mm'}(-\vec{q},q_z), \tag{6}$$

where $M_{nn'}(\vec{q},q_z)$ is the matrix element representing the interaction between the 2D electron gas and 3D phonons, which is defined by

$$M_{nn'}(\vec{q},q_z)=\int_{\infty}^{\infty}dz\,\psi_n(z)V_{\vec{q},q_z}e^{iq_zz}\psi_{n'}(z), \tag{7}$$

where $V_{\vec{q},q_z}$ is the coefficient of the Fourier transform of the Fröhlich Hamiltonian,

$$V_{\vec{q},q_z}=-i\hbar\omega_{\rm LO}\left(\frac{\hbar}{2m^*\omega_{\rm LO}}\right)^{1/4}\sqrt{\frac{4\pi\alpha}{\Omega(q^2+q_z^2)}}, \tag{8}$$

α is the Fröhlich coupling constant, and Ω is the volume of the sample. After some algebra, we obtain

$$v^{\rm ph}_{nn',mm'}(\vec{q},\omega)=\frac{2\pi e^2}{\epsilon_\infty q}\left(\frac{\omega^2_{\rm LO}-\omega^2_{\rm TO}}{\omega^2-\omega^2_{\rm LO}}\right)F_{nn',mm'}(q). \tag{9}$$

The free polarizability function of the Q2D electron gas in the multisubband system, at zero temperature, is given by

$$\Pi^0_{mm'}(\vec{q},\omega)=2\sum_{\vec{k}}\frac{f_{m'}[E_{m'}(\vec{k}+\vec{q})]-f_m[E_m(\vec{k})]}{E_{m'}(\vec{k}+\vec{q})-E_m(\vec{k})+\hbar(\omega+i\gamma)}, \tag{10}$$

where $f(E)$ is the Fermi-Dirac distribution function, and γ is broadening of the energy level related to impurity scattering. When $\gamma\to0$, we obtain[26,28,32]

$$\begin{aligned}{\rm Re}\Pi^0_{mm'}(\vec{q},\omega)=\frac{m^*}{\pi\hbar^2}\Bigg\{&\left[\frac{\nu^-_{mm'}}{2\varepsilon_q}-\frac{1}{\sqrt{\varepsilon_q}}{\rm sgn}(\nu^-_{mm'})\times{\rm Re}(\varepsilon^-_{mm'}-E_{Fm})^{1/2}\right]\Theta(E_{Fm})\\&-\left[\frac{\nu^+_{mm'}}{2\varepsilon_q}-\frac{1}{\sqrt{\varepsilon_q}}{\rm sgn}(\nu^+_{mm'})\times{\rm Re}(\varepsilon^+_{mm'}-E_{Fm'})^{1/2}\right]\Theta(E_{Fm'})\Bigg\}\end{aligned} \tag{11}$$

and

$${\rm Im}\Pi^0_{mm'}(\vec{q},\omega)=-\frac{m^*}{\pi\hbar^2}\{{\rm Re}[4E_{Fm}/\varepsilon_q-(\nu^-_{mm'}/\varepsilon_q)^2]^{1/2}-{\rm Re}[4E_{Fm'}/\varepsilon_q-(\nu^+_{mm'}/\varepsilon_q)^2]^{1/2}\}, \tag{12}$$

where $\varepsilon_q=\hbar^2q^2/2m^*$, $\nu^{\pm}_{mm'}=\hbar\omega+E_{m'}-E_m\pm\varepsilon_q$, $\varepsilon^{\pm}_{mm'}=(\nu^{\pm}_{mm'})^2/4\varepsilon_q$, $E_{Fm}=E_F-E_m$, and $\Theta(E)$ is the step function.

The dielectric function $\epsilon_{nn',ll'}(\vec{q},\omega)$ is defined through the equation $v^{c}_{nn',mm'}(\vec{q})=\Sigma_{ll'}\epsilon_{nn',ll'}(\vec{q},\omega)V^{\rm sc}_{ll',mm'}(\vec{q},\omega)$. When both the electron-electron and the electron-phonon interactions are included in the dielectric function, we obtain within RPA (Ref. 37)

$$\epsilon_{nn',mm'}(q,\omega)=\epsilon_b(\omega)\delta_{nm}\delta_{n'm'}-v^{c}_{nn',mm'}(q)\Pi^0_{mm'}(q,\omega), \tag{13}$$

with

$$\epsilon_b(\omega)=(\omega^2-\omega^2_{\rm LO})/(\omega^2-\omega^2_{\rm TO}). \tag{14}$$

Note that the dielectric function of a 2D electron gas without taking the electron-phonon interaction into account is easily recovered by substituting 1 for $\epsilon_b(\omega)$ in Eq. (13).

The spectrum of collective excitations of the system is given by the zeros of the generalized dielectric function

$$\det|\epsilon_{nn',mm'}(q,\omega)|=0. \tag{15}$$

In principle, all the subbands in the system should be considered in the above equation. If we keep N subbands for numerical calculations, Eq. (15) will be reduced to an $N^2\times N^2$ determinantal equation. In the region where the dielectric function has an imaginary part, i.e., Im $\Pi^0_{mm'}=0$, the plasmon modes are Landau damped. We found that, in the ω-q plane, it corresponds to $\omega^{+}_{nn'}>\omega>\omega^{-}_{nn'}$, with $\omega^{\pm}_{nn'}(q)=(\hbar^2/2m^*)[(q\pm k_{Fn})^2-k^2_{Fn'}]$, where $k_{Fn}=\sqrt{2m^*E_{Fn}}/\hbar$ is the Fermi wave vector of each subband. Notice that the intrasubband plasmon is not damped inside the regime of intersubband single-particle excitations because a charge-density wave parallel to the xy plane cannot excite particles across the subbands.[28]

III. NUMERICAL RESULTS AND DISCUSSIONS

We restrict ourselves to a four-subband model by considering the cases where one, two, or three subbands are occupied by the electrons and we neglect the effect of higher empty subbands.

To begin with, we consider the situation in which only one subband is occupied by the electrons and the other three are empty. There exist plasmon modes denoted by $(1,n')$, where (1,1) is the single intrasubband plasmon mode and those with $n' \geq 2$ represent the intersubband plasmon modes. Within the four-subband model, the intrasubband mode (1,1) and the intersubband mode (1,3) are coupled. The modes are determined by the following dispersion equation (see the Appendix for details):

$$[\epsilon_b(\omega) - v^c_{11,11}(q)\chi^0_{11}(q,\omega)][\epsilon_b(\omega) - v^c_{13,13}(q)\chi^0_{13}(q,\omega)] - v^{c\,2}_{11,13}(q)\chi^0_{11}(q,\omega)\chi^0_{13}(q,\omega) = 0, \quad (16)$$

where $\chi^0_{mm}(q,\omega) = \Pi^0_{mm}(q,\omega)$ and $\chi^0_{mm'}(q,\omega) = \Pi^0_{mm'}(q,\omega) + \Pi^0_{m'm}(q,\omega)$ for $m \neq m'$. On the other hand, the intersubband modes (1,2) and (1,4) are coupled to each other and are given by the solution of

$$[\epsilon_b(\omega) - v^c_{12,12}(q)\chi^0_{12}(q,\omega)][\epsilon_b(\omega) - v^c_{14,14}(q)\chi^0_{14}(q,\omega)] - v^{c\,2}_{12,14}(q)\chi^0_{12}(q,\omega)\chi^0_{14}(q,\omega) = 0. \quad (17)$$

The dispersion relations of the coupled plasmon-phonon modes in a Si δ-doped GaAs system with electron density $N_e = 0.7\times10^{12}$ cm^{-2} are depicted in Fig. 1. In the calculation, we took $\omega_{\rm LO} = 36.25$ meV and $\omega_{\rm TO} = 33.29$ meV. For this density, only the lowest subband is occupied by electrons. The subband Fermi energy $E_{F1} = 22.45$ meV and the subband Fermi wave vector $k_{F1} = 2.03\times10^6$ cm^{-1}. The dispersion relations of the unperturbed plasmon modes without electron-phonon interaction are given by the dashed curves in the figure. Figure 1(a) shows the dispersions of the intrasubband mode (1,1) and the intersubband modes (1,3). The spectrum of the other two modes (1,2) and (1,4) is given in Fig. 1(b). The shadow area corresponds to the single-particle continuum region where Im $\Pi^0_{nn'} \neq 0$. The results of Fig. 1(a) indicate that the dispersion of the unperturbed intrasubband plasmon mode (1,1) develops a loop in the ω-q plane and has an acoustical-like behavior, since ω approaches zero when $q \to 0$. The maximum frequency appears at $(\omega,q) = (35.57,1.23)$ on the edge of the region where Im $\Pi^0_{1,1} = 0$. Hereafter, ω is in energy units meV and q is in units of 10^6 cm^{-1}. In between, there are two frequencies for a given q. The upper branch is located in the region with Im $\Pi_{1,1} = 0$ whereas the lower one is in the region where Im $\Pi_{1,1} \neq 0$ and the collective excitations are strongly Landau damped and are not significant. The above results in the region where the dielectric function has an imaginary part do not exactly correspond to the frequency of the plasmon, which should be determined from the position of the peak in the electron energy-loss function defined as the imaginary part of the inverse of the dielectric function. Nevertheless, it was shown in Ref. 31 that for the plasmon-phonon modes in 2D electron systems, the zeros of the dielectric function correspond to peaks in the energy-loss spectrum. It is seen that the plasmon-phonon coupling is strong for both the intrasubband and the intersubband modes and this shows up at wave vectors far from the resonance where the unperturbed plasmon frequency is close to the LO phonon frequency $\omega_{\rm LO}$.

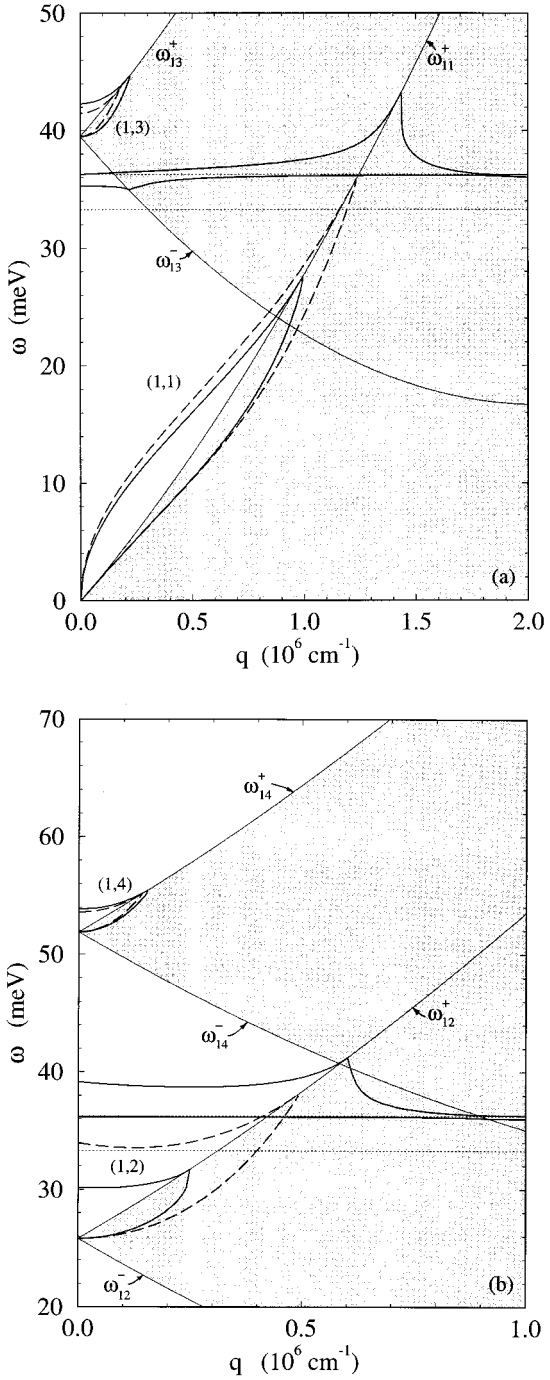

FIG. 1. Dispersions of the collective (a) intrasubband mode (1,1) and the intersubband mode (1,3) and (b) the intersubband modes (1,2) and (1,4) for Si δ-doped GaAs of $N_e = 0.7\times10^{12}$ cm^{-2}. The dispersions of the coupled plasmon-phonon modes and the unperturbed plasmon modes are shown by the thick-solid and the thick-dashed curves, respectively. The thin-solid curves ($\omega^{\pm}_{nn'}$) are the boundaries of the 2D single-particle excitation continuum. The shadow indicates the region where Im$\Pi^0_{nn'} \neq 0$. The dotted lines indicate the optical-phonon frequencies $\omega_{\rm LO}$ and $\omega_{\rm TO}$.

We observe in Fig. 1(a) that the frequency of the unper-

turbed intrasubband plasmon mode (1,1) is smaller than $\omega_{\rm LO}$ for all q. When the electron-phonon interaction is considered, the coupled intrasubband plasmon-phonon modes show two branches in the region where Im $\Pi_{11}^0=0$. The lower branch is shrunk in comparison with the unperturbed plasmon mode, which penetrates into the continuum at $(\omega,q)=(27.20,\ 0.99)$. The upper one is above the LO-phonon frequency. It is very close to $\omega_{\rm LO}$ at $q=0$. By considering the intersubband mode (1,3), we see that the energy difference E_{13} between the two subbands is 39.48 meV, which is greater than $\omega_{\rm LO}$. However, the unperturbed intersubband plasmon frequency is 41.46 meV at $q=0$, which is larger than E_{13} due to the depolarization shift coming from many-body effects. The electron-phonon coupling shifts this intersubband mode to higher frequency. In addition, a phononlike mode appears in the reststrahlen region of GaAs. Figure 1(b) shows the dispersion relations of the intersubband modes (1,2) and (1,4) in the four-subband model when only one subband is occupied. It is seen now that the unperturbed plasmon mode (1,2) crosses the LO-phonon frequency. We observe that the electron-phonon interaction leads to a large splitting of this mode.

Now, we analyze the case where $N_e=2.0\times10^{12}$ cm^{-2} and two subbands of the four-subband model are occupied. The dispersion equations are given by Eqs. (A6) and (A7) in the Appendix. In Fig. 2, we plot the dispersion relations of the coupled plasmon-phonon modes. The subband Fermi energies are $E_{F1}=50.41$ meV and $E_{F2}=11.24$ meV, respectively. Consequently, $k_{F1}=3.04\times10^6$ cm^{-1} and $k_{F2}=1.42\times10^6$ cm^{-1}. Figure 2(a) shows the dispersion of the coupled modes (1,1), (2,2), (1,3), and (2,4). The dashed curves in the figure indicate the dispersion relations of the plasmon modes without the electron-phonon interaction. By comparing with the results shown in Fig. 1(a), we observe that two extra plasmon modes (2,2) and (2,4) arise due to the occupation of the $n=2$ subband. Furthermore, the increase of the total electron density (doping concentration) leads to higher subband electron density and larger separation in energy between two subbands. Due to the higher electron density (larger Fermi wave vector) in the lowest subband, the unperturbed intrasubband plasmon mode (1,1) crosses over the LO-phonon frequency, and the electron-phonon interaction leads to the splitting of this mode. We see that the intrasubband mode (2,2) is not so pronounced and it is located within the single-particle continuum of the lowest subband. The intersubband mode (2,4) is close to, but smaller than, the phonon frequency $\omega_{\rm LO}$. The shrink of this mode is pronounced due to the electron-phonon coupling. Contrary to the situation shown in Fig. 1(a), the effect of the electron-phonon coupling on the intersubband mode (1,3) is not significant since its frequency is much larger than $\omega_{\rm LO}$ in the present case. In Fig. 2(b) the most significant effect of the electron-phonon interaction is shown on the intersubband plasmon mode (1,2). The electron-phonon coupling leads to a shift of this mode to higher frequency and another phononlike mode appears in the reststrahlen region. This phononlike mode is almost flat.

Finally, we analyze the case where the electron density $N_e=5.0\times10^{12}$ cm^{-2} which corresponds to three occupied subbands. Here, the subband Fermi energies (Fermi wave vectors) are $E_{F1}=100.89$ meV ($k_{F1}=4.31\times10^6$ cm^{-1}),

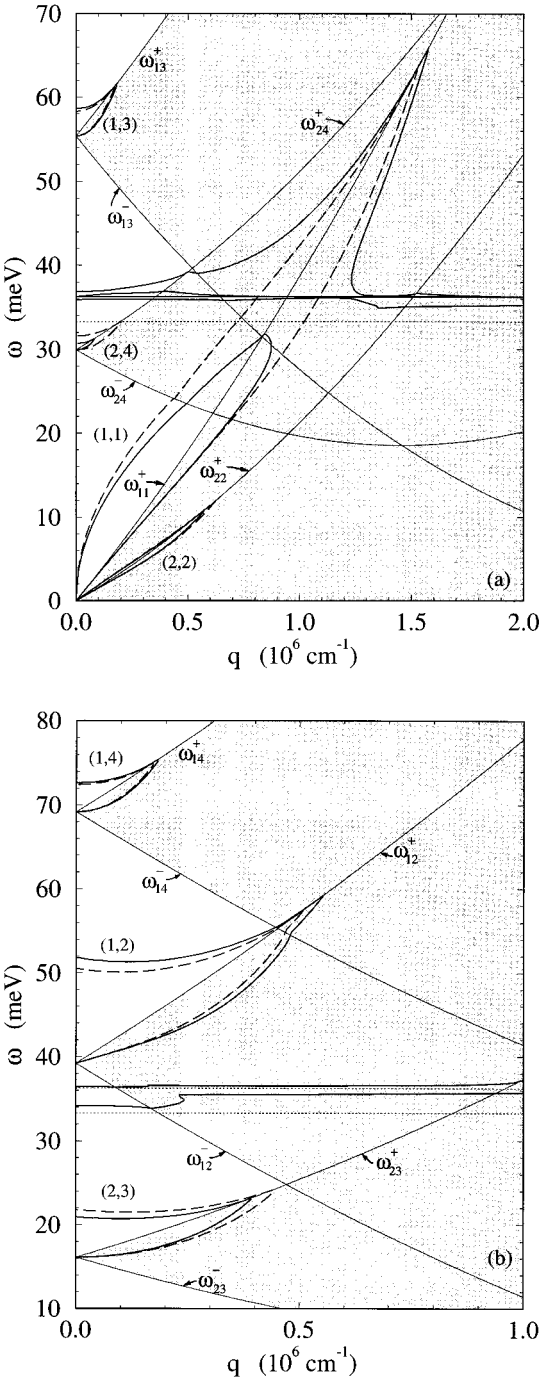

FIG. 2. The same as Fig. 1 but now for $N_e=2\times10^{12}$ cm^{-2}. Four plasmon modes (1,1), (2,2), (1,3), and (2,4) appear in (a) and three plasmon modes (1,2), (2,3), and (1,4) in (b).

$E_{F2}=33.23$ meV ($k_{F2}=2.47\times10^6$ cm^{-1}), and $E_{F3}=8.82$ meV ($k_{F3}=1.27\times10^6$ cm^{-1}), respectively. Figure 3 shows the dispersion relations of the coupled plasmon-phonon modes. Two additional plasmon modes are found: the intrasubband mode (3,3) shown in Fig. 3(a) and the intersubband mode (3,4) in Fig. 3(b). The intrasubband mode (1,1) in Fig. 3(a) is strongly coupled to the LO-phonon modes. The coupling of the intersubband mode (2,4) to the LO-phonon leads to a phononlike mode in the reststrahlen region starting from $\omega=35.11$ meV at $q=0$. In Fig. 3(b), the electron-phonon

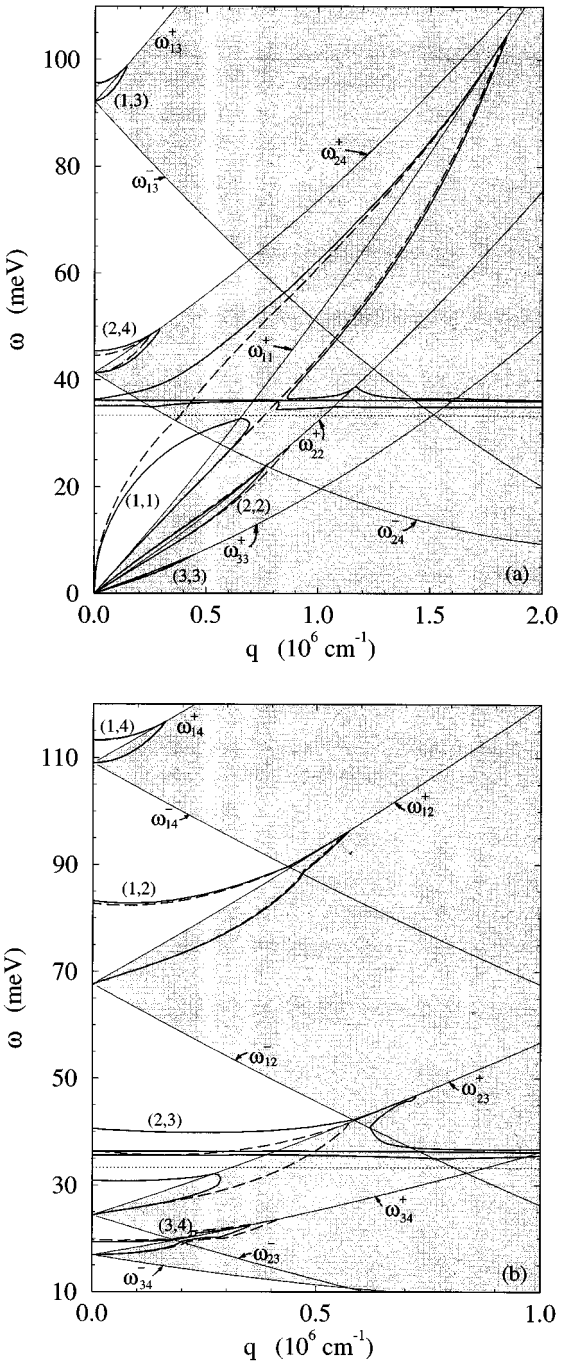

FIG. 3. The same as Fig. 1 but now for $N_e = 5\times10^{12}$ cm^{-2}. Five plasmon modes (1,1), (2,2), (3,3), (1,3), and (2,4) appear in (a) and four plasmon modes (1,2), (1,4), (2,3), and (3,4) in (b).

coupling results in a pronounced splitting of the intersubband mode (2,3).

In Fig. 4, the unperturbed intersubband plasmon frequencies at $q = 1\times10^4$ cm^{-1} are plotted as a function of the total electron density in the δ-doped system. The dotted curves represent the energy difference $E_{n'} - E_n$ between the two subbands. We see that, at the onset of the occupation of a subband, the intersubband plasmon frequency is equal to the energy difference. By increasing the total electron density, and the subband electron density, the intersubband plasmon frequency becomes larger than the energy difference. This

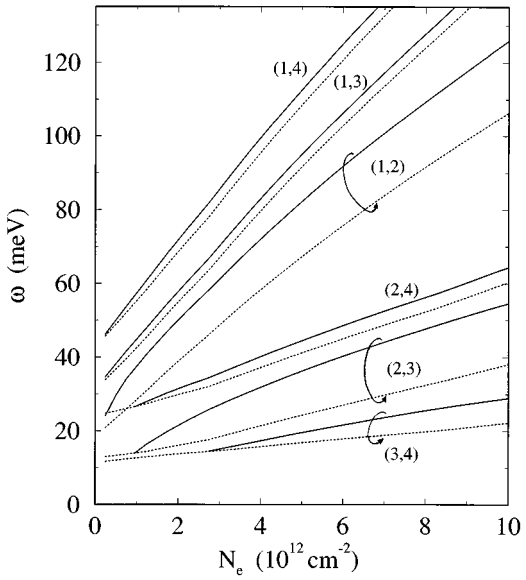

FIG. 4. The unperturbed intersubband plasmon frequencies at $q = 10^4$ cm^{-1} as a function of the total electron density in Si δ-doped GaAs. The dotted curves indicate the energy differences between the subbands.

results in a depolarization shift due to many-body effects. The shift is more pronounced for adjacent subbands, i.e., the intersubband modes (1,2) and (2,3). When the electron-phonon interaction is included, the intersubband plasmon frequency splits around the LO-phonon frequency. The frequencies of the coupled plasmon-phonon modes at $q = 1\times10^4$ cm^{-1}, as a function of the total electron density, are depicted in Fig. 5(a) for the (1,2) and (1,3) intersubband modes and in Fig. 5(b) for the (2,3) and (2,4) modes. The thin curves represent the corresponding intersubband plasmon frequencies without the electron-phonon interaction. We see that the intersubband plasmon modes are strongly coupled to the optical-phonon modes. When the unperturbed intersubband frequency is equal to $\omega_{\rm LO}$, the splitting is 9.29 meV for the (1,2) mode and 9.73 meV and 5.45 meV for (2,3) and (2,4) modes, respectively. At low electron densities, the lower branch is close to the unperturbed plasmon frequency and it is much smaller than $\omega_{\rm LO}$, while the frequencies of the upper branch are close to $\omega_{\rm LO}$. However, the lower branch approaches the $\omega_{\rm LO}$ at high densities whereas the upper one becomes close to the unperturbed plasmon frequency. For a wide range of electron densities, the frequencies of the lower branch of the intersubband plasmon-phonon modes (1,3), (1,2), and (2,4) lie in the reststrahlen region of GaAs.

The coupled plasmon-phonon mode in the reststrahlen region was observed experimentally for the Si δ-doped GaAs system by Mlayah *et al.*[9] They found in the Raman spectrum that the phononlike mode appears at $\omega = 34.97$ meV (282 cm^{-1}) for the sample with donor concentration $N_D = 2.7\times10^{12}$ cm^{-2} and $W_D \simeq 20$ Å. By fitting the Raman spectrum, they obtained the depolarization shift about 26.67 meV (215 cm^{-1}) for the unperturbed intersubband mode (1,2). From our calculation with the same donor concentration, we obtained for the intersubband mode (1,2) ($E_{12} = 42.09$ meV), the unperturbed plasmon frequency

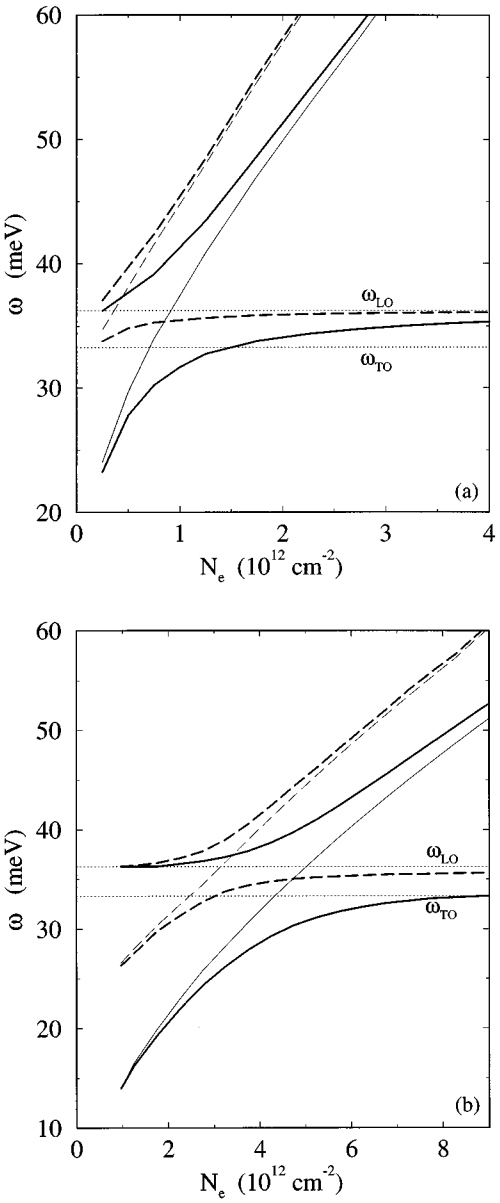

FIG. 5. The frequencies of the coupled intersubband plasmon-phonon modes (a) (1,2) (solid curves) and (1,3) (dashed curves) and (b) (2,3) (solid curves) and (2,4) (dashed curves) at $q=10^4\ \mathrm{cm}^{-1}$ as a function of electron density. The thin curves indicate the unperturbed plasmon frequency.

equals to 54.21 meV, a depolarization shift of 34.08 meV, and frequencies of the coupled plasmon-phonon modes with values 34.28 meV and 55.54 meV. So, our results are in reasonable agreement with the experimental results of Ref. 9. However, we also observed that, for higher electron densities, there are two or more intersubband plasmon-phonon modes in the reststrahlen region such as (1,2), (1,3), and (2,4) modes. At $N_e > 8\times10^{12}\ \mathrm{cm}^{-2}$, the intersubband mode (2,3) would play an important role in this region.

IV. CONCLUSIONS

We have calculated the spectrum of the coupled plasmon-phonon modes for a multisubband electron system realized in Si δ-doped GaAs. The numerical results show that the electron-phonon interaction alters the unperturbed plasmon-excitation spectrum considerably. Due to its high electron density, the plasmon-phonon coupling is substantially stronger than that in other 2D systems, such as semiconductor quantum wells and heterojunctions. Since several subbands are occupied by the electrons, the intersubband plasmon modes have be shown to be essential to the physical description of the system.

Our results show that the high electron density leads to a large depolarization shift of the intersubband plasmon frequencies between adjacent subbands. Furthermore, both intrasubband plasmon and intersubband plasmon modes are strongly coupled to the optical-phonon modes. The frequencies of the coupled intrasubband plasmon-phonon modes do not enter in the reststrahlen region of GaAs. However, the frequencies of the coupled intersubband plasmon-phonon modes split around the LO-phonon frequency ω_{LO}. In a wide range of electron density (donor concentration), the frequencies of the phononlike branch of the intersubband plasmon-phonon modes (1,2), (1,3), (2,3), and (2,4) are in the reststrahlen region of GaAs.

ACKNOWLEDGMENTS

This work was partially sponsored by the Conselho Nacional de Desenvolvimento Científico e Tecnológico (CNPq) and the Fundação de Amparo à Pesquisa do Estado de São Paulo (FAPESP). G.Q.H. is supported by CNPq (Brazil).

APPENDIX

In this appendix, we show in detail how the determinantal equation for the dielectric matrix, Eq. (15), was solved numerically. Due to the symmetry of the confinement potential in the δ-doped system which results in the vanishing of the form factor $F_{nn',mm'}(q)$, given by Eq. (5), when $n+n'+m+m'$ is an odd number, and the corresponding matrix elements of the dielectric function, given by Eq. (13), we find that there are two groups of plasmon modes. One of them includes all the intrasubband modes as well as the intersubband modes whose wave functions have the same parity. All plasmon modes in this group are coupled to each other. The other group is formed by the intersubband modes of two subbands with different parities and the plasmon modes in this group are also coupled to each other but they do not interact with the modes of the former one.

In the four-subband model, the 16×16 determinantal equation is reduced to the following two groups of equations:

$$\begin{vmatrix} \kappa_{11,11} & \kappa_{11,22} & \kappa_{11,33} & \kappa_{11,44} & \kappa_{11,13} & \kappa_{11,24} \\ \kappa_{22,11} & \kappa_{22,22} & \kappa_{22,33} & \kappa_{22,44} & \kappa_{22,13} & \kappa_{22,24} \\ \kappa_{33,11} & \kappa_{33,22} & \kappa_{33,33} & \kappa_{33,44} & \kappa_{33,13} & \kappa_{33,24} \\ \kappa_{44,11} & \kappa_{44,22} & \kappa_{44,33} & \kappa_{44,44} & \kappa_{44,13} & \kappa_{44,24} \\ \kappa_{13,11} & \kappa_{13,22} & \kappa_{13,33} & \kappa_{13,44} & \kappa_{13,13} & \kappa_{13,24} \\ \kappa_{24,11} & \kappa_{24,22} & \kappa_{24,33} & \kappa_{24,44} & \kappa_{24,13} & \kappa_{24,24} \end{vmatrix} = 0 \tag{A1}$$

and

$$\begin{vmatrix} \kappa_{12,12} & \kappa_{12,14} & \kappa_{12,23} & \kappa_{12,34} \\ \kappa_{14,12} & \kappa_{14,14} & \kappa_{14,23} & \kappa_{14,34} \\ \kappa_{23,12} & \kappa_{23,14} & \kappa_{23,23} & \kappa_{23,34} \\ \kappa_{34,12} & \kappa_{34,14} & \kappa_{34,23} & \kappa_{34,34} \end{vmatrix} = 0 , \tag{A2}$$

where

$$\kappa_{nn',mm'}(q,\omega) = \epsilon_b(\omega)\delta_{nm}\delta_{n'm'} - v^c_{nn',mm'}(q)\chi^0_{mm'}(q,\omega), \tag{A3}$$

with $\chi^0_{mm}(q,\omega) = \Pi^0_{mm}(q,\omega)$ and $\chi^0_{mm'}(q,\omega) = \Pi^0_{mm'}(q,\omega) + \Pi^0_{m'm}(q,\omega)$ for $m \neq m'$.

In the case of only one occupied subband, Eqs. (A1) and (A2) reduce to

$$\begin{vmatrix} \kappa_{11,11} & \kappa_{11,13} \\ \kappa_{13,11} & \kappa_{13,13} \end{vmatrix} = 0 \tag{A4}$$

and

$$\begin{vmatrix} \kappa_{12,12} & \kappa_{12,14} \\ \kappa_{14,12} & \kappa_{14,14} \end{vmatrix} = 0. \tag{A5}$$

It is seen that the intrasubband mode (1,1) couples to the intersubband mode (1,3) determined by Eq. (A4). The other two intersubband modes (1,2) and (1,4) are coupled to each other.

In the case of two occupied subbands within the four-subband model, the determinantal equations, given by Eqs. (A1) and (A2), are now written in terms of 4×4 and 3×3 determinants. There are two intrasubband modes (1,1) and (2,2). These two modes are coupled to each other and also coupled to the intersubband modes (1,3) and (2,4). They are determined by the dispersion equation

$$\begin{vmatrix} \kappa_{11,11} & \kappa_{11,22} & \kappa_{11,13} & \kappa_{11,24} \\ \kappa_{22,11} & \kappa_{22,22} & \kappa_{22,13} & \kappa_{22,24} \\ \kappa_{13,11} & \kappa_{13,22} & \kappa_{13,13} & \kappa_{13,24} \\ \kappa_{24,11} & \kappa_{24,22} & \kappa_{24,13} & \kappa_{24,24} \end{vmatrix} = 0. \tag{A6}$$

The remaining coupled intersubband modes (1,2), (2,3), and (1,4) can be calculated from

$$\begin{vmatrix} \kappa_{12,12} & \kappa_{12,14} & \kappa_{12,23} \\ \kappa_{14,12} & \kappa_{14,14} & \kappa_{14,23} \\ \kappa_{23,12} & \kappa_{23,14} & \kappa_{23,23} \end{vmatrix} = 0. \tag{A7}$$

In the case of three occupied subbands, Eq. (A1) reduces to

$$\begin{vmatrix} \kappa_{11,11} & \kappa_{11,22} & \kappa_{11,33} & \kappa_{11,13} & \kappa_{11,24} \\ \kappa_{22,11} & \kappa_{22,22} & \kappa_{22,33} & \kappa_{22,13} & \kappa_{22,24} \\ \kappa_{33,11} & \kappa_{33,22} & \kappa_{33,33} & \kappa_{33,13} & \kappa_{33,24} \\ \kappa_{13,11} & \kappa_{13,22} & \kappa_{13,33} & \kappa_{13,13} & \kappa_{13,24} \\ \kappa_{24,11} & \kappa_{24,22} & \kappa_{24,33} & \kappa_{24,13} & \kappa_{24,24} \end{vmatrix} = 0 , \tag{A8}$$

while Eq. (A2) keeps the same form.

[1] E. F. Schubert, in *Semiconductors and Semimetals*, edited by A. C. Gossard (Academic Press, New York, 1994), Vol. 40, p. 1.

[2] S. J. Bass, J. Cryst. Growth **47**, 613 (1979).

[3] C. E. C. Wood, G. M. Metze, J. D. Berry, and L. F. Eastman, J. Appl. Phys. **51**, 383 (1980).

[4] E. F. Schubert, J. B. Stark, B. Ullrich, and J. E. Cunningham, Appl. Phys. Lett. **52**, 1508 (1988).

[5] P.M. Koenraad, in *Delta Doping of Semiconductors*, edited by E.F. Schubert (Cambridge Univ. Press, London, 1995), p. 304.

[6] A. Zrenner, F. Koch, J. Leotin, M. Goiran, and K. Ploog, Semicond. Sci. Technol. **3**, 1132 (1988).

[7] E. Skuras, R. Kumar, R. L. Williams, R. A. Stradling, J. E. Dmochowski, E. A. Johnson, A. Mackinnon, J. J. Harris, R. B. Beall, C. Skierbeszewski, J. Singleton, P. J. van der Wel, and P. Wisnieski, Semicond. Sci. Technol. **6**, 535 (1991).

[8] J. J. Harris, R. Murray, and C. T. Foxon, Semicond. Sci. Technol. **8**, 31 (1993).

[9] A. Mlayah, R. Carles, E. Bedel, and A. Muñoz-Yagüe, Appl. Phys. Lett. **62**, 2848 (1993); J. Appl. Phys. **74**, 1072 (1993).

[10] C. Lohe, A. Leuther, A. Förster, and H. Lüth, Phys. Rev. B **47**, 3819 (1993).

[11] Yu. A. Pusep, M. T. O. Silva, J. C. Galzerani, S. W. da Silva, L. M. R. Scolfaro, R. Enderlein, A. A. Quivy, A. P. Lima, and J. R. Leite, Phys. Rev. B **54**, (to be published).

[12] G. Hasnain, G. H. Döhler, J. R. Whimery, J. N. Miller, and A. Dienes, Appl. Phys. Lett. **49**, 1357 (1986).

[13] E. F. Schubert, J. P. van der Ziel, J. E. Cunningham, and T. D. Harris, Appl. Phys. Lett. **55**, 757 (1989).

[14] E. F. Schubert and J. E. Cunningham, Electron. Lett. **24**, 980 (1988).

[15] E. F. Schubert, J. E. Cunningham, W. T. Tsang, and G. L. Timp, Appl. Phys. Lett. **51**, 1170 (1987).

[16] R. J. Malik, T. R. AuCoin, R. L. Ross, K. Board, C. E. C. Wood, and L. F. Eastman, Electron. Lett. **16**, 836 (1980).

[17] J. N. Bailargeon, K. Y. Cheng, J. Lasker, and J. Kolodzey, Appl Phys. Lett. **55**, 663 (1989).

[18] G. Abstreiter, M. Cardona, and A. Pinczuk, in *Light Scattering in Solids IV*, edited by M. Cardona and G. Güntherodt (Springer-Verlag, Berlin, 1984), p. 36.

[19] E. Burnstein, A. Pinczuk, and S. Bucher, in *Physics of Semiconductors*, edited by B. L. H. Wilson (The Institute of Physics, London, 1979), p. 1231; E. Burstein, A. Pinczuk, and D. L. Mills, Surf. Sci. **98**, 451 (1980).

[20] D. Olego, A. Pinczuk, A. C. Gossard, and W. Wiegmann, Phys. Rev. B **25**, 7867 (1982); R. Sooryyakumer, A. Pinczuk, A. C. Gossard, and W. Wiegmann, *ibid.* **29**, 3318 (1984).

[21] A. Pinczuk, M. G. Lamont, and A. C. Gossard, Phys. Rev. Lett. **56**, 2092 (1986).

[22] G. Fasol, N. Mestres, H. P. Hughes, A. Fischer, and K. Ploog, Phys. Rev. Lett. **56**, 2517 (1986).

[23] J. W. Wu, P. Hawrylak, and J. J. Quinn, Phys. Rev. Lett. **55**, 879 (1985).

[24] J. K. Jain and P. B. Allen, Phys. Rev. Lett. **54**, 947 (1984); **55**, 997 (1985).

[25] S. Das Sarma, A. Kobayashi, and R. E. Prange, Phys. Rev. Lett. **56**, 1280 (1986); Phys. Rev. B **34**, 5309 (1986).
[26] X. Wu and S. E. Ulloa, Phys. Rev. B **48**, 14 407 (1993).
[27] S. Das Sarma, Phys. Rev. B **29**, 2334 (1984).
[28] J. K. Jain and S. Das Sarma, Phys. Rev. B **36**, 5949 (1987).
[29] Q. Li and S. Das Sarma, Phys. Rev. B **40**, 5860 (1989); **43**, 11 768 (1991).
[30] W. H. Backes, F. M. Peeters, F. Brosens, and J. T. Devreese, Phys. Rev. B **45**, 8437 (1992).
[31] X.-G. Wu, F. M. Peeters, and J. T. Devreese, Phys. Rev. B **32**, 6982 (1985).
[32] L. Wendler and R. Pechstedt, Phys. Status Solidi B **138**, 197 (1986); **141**, 129 (1987).
[33] G.-Q. Hai, F. M. Peeters, and J. T Devreese, Phys. Rev. B **42**, 11 063 (1990); **47**, 10 358 (1993).
[34] G.-Q. Hai and N. Studart, Phys. Rev. B **52**, R2245 (1995).
[35] G.-Q. Hai, N. Studart, and F. M. Peeters, Phys. Rev. B **52**, 8363 (1995).
[36] G.-Q. Hai, N. Studart, F.M. Peeters, P. M. Koenraad, and J. H. Wolter, J. Appl. Phys. (to be published).
[37] G. D. Mahan, *Many-Particle Physics* (Plenum Press, New York, 1981).
[38] M. Jonson, J. Phys. C **9**, 3055 (1976); P. J. Price, Phys. Rev. B **30**, 2234 (1984); U. de Freitas and N. Studart, *ibid.* **36**, 6677 (1987).